

# Clay minerals in historic buildings

Veridiana Reyes-Zamudio · Carlos Angeles-Chávez ·  
Jorge Cervantes

Cultural heritage special chapter  
© Akadémiai Kiadó, Budapest, Hungary 2010

**Abstract** Although identified in heritage stones, clays are not always taken into full account in terms of negative effects due to their swelling ability (Delgado Rodrigues, *Materiales de Construcción* 51:183–195, 2001). The main purpose of this study is to identify clays in welded tuffs of three different historic monuments located in the city of Guanajuato, Mexico, and to establish the clays' contribution to the deterioration of the monuments by their swelling behavior. Thermal analysis, differential thermal analysis (DTA), thermogravimetry (TG), and dynamic mechanical analysis (DMA), as well as supplementing data with X-ray diffraction (XRD), Fourier transform infrared spectroscopy (FTIR), and environmental scanning electron microscopy (ESEM), have been used. Data suggest that clays present in welded tuffs of the historic monuments studied contribute to increased deterioration through osmotic swelling in two of the three monuments.

**Keywords** Clay minerals · Cultural stone · Ignimbrites · Monuments · Swelling · Volcanic tuff

## Introduction

Volcanic tuffs, one type of volcanic stones, are present in many monuments around the world, from sculptures to

buildings. In Latin America, volcanic tuffs were used extensively, for example, in pyramids, monoliths, and colonial churches [1]. These stones are formed by the solidification of magma fragments of different sizes (pyroclastic material) that are transported through the atmosphere. As a result, they are stones with heterogeneous compositions of crystalline minerals (quartz or their polymorphs, feldspars, micas, etc.) and volcanic glass [2].

In general, volcanic stones are not chemically stable in wet acid conditions at ambient temperature [3]. The influence of CO<sub>2</sub> and SO<sub>2</sub> on the deterioration of this kind of stone has been reported [4–7]. One of the main weathering processes is the dissolution of feldspars and volcanic glass and the formation of secondary clay minerals such as halloysite, smectite, illite, allophane, and kaolinite [8, 9]. This also includes secondary assemblages such as kaolinite–halloysite, kaolinite–smectite, and illite–smectite, which depend on local physicochemical conditions due to the particular rock fabric [10–12].

Clay minerals, either diffused throughout the stone framework or as coating-filling of void spaces, can play an important role in stone damage [13]. It is considered that scaling and flaking, typical forms of deterioration of volcanic tuffs, are especially severe when clay minerals are present [9]. The harmful role of clays derives from their capacity to induce mechanical stresses inside the stone skeleton. This is a result of a swelling/shrinking process induced by continuous changes in humidity and temperature which lead to the formation of microcracks and detachment of superficial stone flakes [13, 14]. The swelling/shrinking cycles cause havocs in areas free of pressure such as capitals, columns, arches, vaults, cornices, etc.

Swelling is associated with two distinct processes in clays: intra- and interparticle swelling [14]. Intraparticle or intracrystalline swelling is an increase of interlayer space

---

V. Reyes-Zamudio · J. Cervantes (✉)  
Departamento de Química, D.C.N.E.,  
Universidad de Guanajuato, Noria Alta s/n,  
C.P. 36050 Guanajuato, GTO, Mexico  
e-mail: jauregi@quijote.ugto.mx

C. Angeles-Chávez  
Instituto Mexicano del Petróleo,  
Eje Central Norte Lázaro Cárdenas 152, Col. San Bartolo  
Atepehuacan, C.P. 07730 Mexico City, Mexico

of crystal-chemical units when a polar liquid (e.g., water or ethylene glycol) fits in this space due to the presence of counter ions. This phenomenon is particular to smectite, vermiculite, illite, and chlorite. Interparticle or osmotic swelling is the result of the repulsive forces between charged surfaces generated by the removal by osmosis of ions between them. It is experienced by all clay minerals (expandable and non-expandable clays) in the presence of water and electrolytes [13, 15, 16]. The swelling characteristics of different clays are related to their chemical composition and also to the kind and degree of isomorphous substitutions in their layers and the amount and nature of their exchangeable cations [17]. On the other hand, the expansion produced by osmotic swelling is greater than the intracrystalline swelling [18].

The swelling strain is the length (in mm/m) that the stone expands when it is placed in contact with water. The efforts generated in the stone due to wetting/drying events are proportional to swelling strain. In general, swelling strain values above 1.5 mm/m can be considered quite large; however, minor values can cause damage depending on the particular resistance of each stone [15]. A way of preventing the damage by wetting/drying cycles is to reduce the swelling strain of the material [18].

The management of the swelling problem has a longer tradition in current geotechnical works than in the conservation of the built heritage field. The characterization of cultural stones in connection with this phenomenon has been the focus of more attention until recent years [19–21].

On the other hand, clays may have an influence on the capability of stones to be consolidated with alkoxysilanes [22], the most common product used in the consolidation of silicate stone-based monuments. Some authors report the harmful effects in consolidated stones with contents of expandable clays [23, 24]. The use of surfactants and other pre-treatments have been reported to avoid the expansion of clays before the consolidation process takes place [25].

Guanajuato is among the Mexican cities designated World Cultural Heritage Sites by UNESCO. The city has many historic buildings constructed mainly in the seventeenth, eighteenth, and nineteenth centuries. As in central-western Mexico, in the city of Guanajuato most of the statuary and facades of colonial churches or civil buildings were carved on welded tuffs (ignimbrites), one of the most common volcanic tuffs used as building material [1].

The aim of this study is to identify and characterize the content of clays in samples of welded tuffs from three different historic monuments of the city of Guanajuato, and to establish the clays' contribution to the deterioration of these monuments, using thermal analysis techniques [differential thermal analysis (DTA), thermogravimetry (TG),

and dynamic mechanical analysis (DMA)] and supplementing the information with X-ray diffraction (XRD), Fourier transform infrared spectroscopy (FTIR), and environmental scanning electron microscopy (ESEM).

## Experimental

### Materials

The stone materials were obtained from three different important buildings of the city of Guanajuato, all constructed with pink welded tuffs (ignimbrites) called in Mexico “cantera rosa.” Given the patrimonial character of the monuments, only small amounts of sample, but enough for all the analyses, were taken during recent conservation works done in the buildings. The samples have been named Basilica, College, and Rocha.

The Basilica monument is the principal church of the city. It is located in downtown Guanajuato and is the center of the religious life of the city because the church holds the Virgin Mary image known as Our Lady of Guanajuato. The building was built from 1671 to 1696. Multiple stages of construction were necessary, and, as a result, the church shows various architectural styles: baroque, neoclassical, and eclectic. The sample was taken from the baroque clock tower, which was finished in 1776. The clock tower, like the facade and many monuments in Mexico, was initially covered with mortar and painted. It is not known if this coating was rasped during the movement ordered by the government at the beginning of the twentieth century, or if it has been lost little by little. Some vestiges are still present. It is important to point out that this part of the building is one of the most deteriorated, presenting cracking, flaking, and spalling. The stone employed to build the tower came from a different ore than the one used in the construction of the church facades.

The Teachers College is a civil building located on one of the highly trafficked streets in the town. This building was initially built as a summer residence at the end of the nineteenth century; in 1940, it was renovated and used as a hospital. In 1953, it was refurbished to host the State Teachers College, which remains its current function. It is a neoclassical building, and all of its facades were built with pink welded tuff. The sample of this monument came from one of the cornices that was replaced during the last restoration works of the building. Before the restoration, the cornices showed fractures, spalling, and the loss of large sections.

The Monument to General Sóstenes Rocha is located on the same street as the Teachers College, close to a park and surrounded by a small garden. The monument was inaugurated in 1955. It consists of a brass sculpture on a

neoclassical base carved in pink tuff. The base was very deteriorated and showed spalling, flaking, fractures, and loss of material. The sample came from one of these pieces that fell from the monument. Recently, the monument was restored by replacing almost all the stone that makes up the base.

## Methods

### Bulk samples

The samples were divided in three portions: one portion was powdered in an agate mortar to pass a 100-mesh sieve for the thermal analysis studies (DTA and TG) and XRD. Another portion was used in the swelling measurements. The rest was employed to separate the clay fraction.

### Separation of clay fractions

The samples were pulverized in an agate mortar to pass a 200-mesh sieve. Approximately 5 g were treated with 1 M acetic acid, and the insoluble residue was washed repeatedly with distilled water. The clay fractions were separated by sedimentation and dried at 80 °C. These fractions were analyzed by DTA and TG, XRD, FTIR, and ESEM.

### Instrumentation

Powder XRD data were collected on a Siemens D500 powder X-ray diffractometer using  $\text{CuK}\alpha$  radiation. The data were collected from 2 to 65° 2 $\theta$ . All samples were obtained on random mounts. The DTA and TG/DTG curves were determined simultaneously by a TA Instruments SDT-Q600 Simultaneous TG-DSC unit, at the heating rate of 10 °C min<sup>-1</sup>, using  $\alpha\text{-Al}_2\text{O}_3$  as a reference material, under nitrogen dynamic atmosphere. The sample size analyzed was 10 mg in platinum crucibles. The temperature range was from ambient to 1050 °C. The infrared transmittance spectra were obtained using a Perkin Elmer Spectrum 100 FTIR spectrometer; KBr disks were prepared in a sample/KBr proportion of 1/1000. For the observations by ESEM, a Philips XL 30 instrument was used. Three repeated experiments were performed for DTA, TG, XRD, and FTIR for each sample. No considerable differences were observed between them.

Measurements of swelling were performed on a Perkin Elmer DMA 7. Linear expansion was measured as a function of time after the addition of distilled water on samples, ranging from 7 to 10 mm in height and 3 × 3 mm in cross section. Swelling strains were measured perpendicularly to bedding planes. The reported values are the average of three measurements.

## Results

### XRD analysis

Quartz, albite, anortite, and orthoclase are the dominant minerals in the three samples. Small broad signals of regular alternating illite and montmorillonite layers, rectorite  $d_{001}$  25.8 Å, were obtained in College and Rocha samples. The Basilica sample did not present signs of clays. Calcite was identified in Basilica and College. The results of the XRD analysis on the bulk stones confirm the mineralogy determined previously by petrography [26].

The patterns of the clay fractions in the College and Rocha samples presented a mixture of signals that correspond mainly to rectorite,  $d_{001}$  25.8 Å, and bentonite,  $d_{001}$  12.2 Å, while in Basilica very broad signals identified as rectorite,  $d_{001}$  25.8 Å, and sodium montmorillonite,  $d_{001}$  14.7 Å, were obtained. In addition, the clay fractions showed peaks for quartz, albite, and orthoclase.

### DTA

#### Bulk samples

The experimental curves of the DTA of each of the three bulk samples are presented in Fig. 1. In general, the curves for Basilica and College were very similar, with some differences observed with respect to the Rocha curve. Basilica and College showed a fairly typical curve for montmorillonite, two endothermic reactions centered at 140 and 650 °C, one shoulder at 750 °C, and a small exothermic peak at 1015 °C. The small peaks on curves at about 560 °C could be assigned to a small amount of kaolinite and quartz.

The College sample presented another endothermic peak centered at 670 °C, corresponding to the decomposition of calcium carbonate, already detected by XRD. The temperature of decomposition attributed to the finer particle size of calcite due to its origin, the weathering of feldspars, and observed previously by petrography [26]. This is also

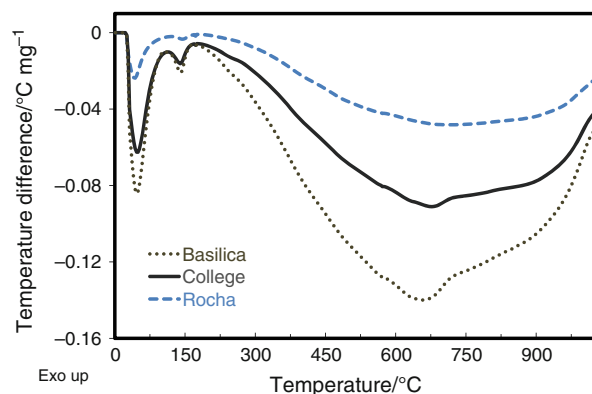


**Fig. 1** DTA curves of the bulk samples

in agreement to the observations of Shoval et al. [27], Cardiano et al. [28], and Duran et al. [29]. They found that calcite materials can decompose in a wide range of temperature, starting below 650 °C (assigned to the de-carbonation of polycrystalline calcite), to nearly 850 °C (attributed to the total decomposition of monocrystalline calcite).

The Rocha sample showed a curve with wide and poorly defined peaks corresponding to amorphous material. The curve has three endothermic reactions centered at 142, 554, and 683 °C, shoulders centered at 400, 491, and 888 °C, and a small exothermic reaction centered at 999 °C.

### Clay fractions

The general shape of the DTA curves of the clay fractions did not change with respect to the curves of the bulk samples. However, there was a slight increase in temperatures of the maximum peaks of dehydroxylation reactions of the clays, due to the absence of carbonates. In general, it was confirmed that the Basilica and College samples presented a very similar thermal behavior. The reaction temperatures in the total range analyzed coincide almost exactly, only varying in signal intensity; except for the dehydroxylation reaction of montmorillonite, which occurred at a higher temperature in the sample College. These samples showed thermal reactions similar to the values reported for the cheto type montmorillonite [30]: three endothermic reactions at 137, 666, and 877 °C and an exothermic reaction at 1011 °C.

On the other hand, the Rocha sample presents the same shape as the bulk sample, without maximum peaks and poorly defined.

### TG-DTG

In comparing the curves of the clay fractions presented in Fig. 2, it is clear that the samples contain more than one phase. So, the three clay fractions are in reality a mixture of the same phases but in different proportions. However, when comparing these curves with the curves obtained for the bulk samples after treatment with 1 M acetic acid, Fig. 3, it is observed that the College clay fraction has a higher concentration of montmorillonite. Therefore, mass losses were calculated in these curves taking into account the decomposition ranges presented in the clay fraction curves, Table 1.

Although identified by XRD rectorite phase, in the three clay fraction samples, the thermal behavior of the samples does not correspond to the standard reference rectorite Rar-1 thermal behavior.

Clay percentages calculated based on dry weight are presented in Table 2. The amount of each clay in the samples was determined using the mass loss from dehydroxylation and assuming ideal hydroxyl water content of 5% for montmorillonite, 14% for halloysite and kaolinite, and 4% for illite.

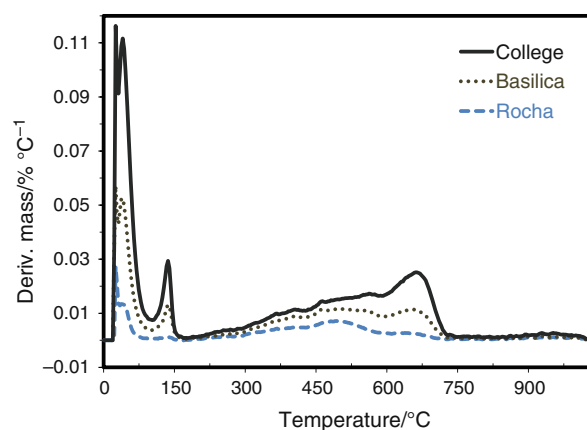


**Fig. 2** DTG curves of the clay fractions

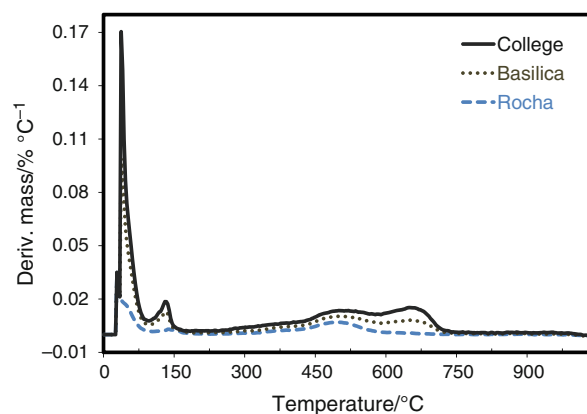


**Fig. 3** DTG curves of the bulk samples after treatment with 1 M acetic acid

**Table 1** Decomposition regions and % mass losses of the bulk samples after treatment with 1 M acetic acid

Decomposition regions	% Mass losses		
	Basilica	College	Rocha
30–165 °C	1.7	1.2	1.0
Water adsorbed on the surfaces			
165–331 °C	0.19	0.3	0.1
Interlayer water of montmorillonite			
331–431 °C	0.16	0.16	0.23
Dehydroxylation of illite			
431–516 °C	0.21	0.27	0.49
Dehydroxylation of halloysite			
516–588 °C	0.32	0.26	0.26
Dehydroxylation of kaolinite			
588–732 °C	0.71	0.72	0.1
Dehydroxylation of montmorillonite			

**Table 2** Clay composition of the bulk samples after treatment with 1 M acetic acid, % mass

	Illite	Halloysite	Kaolinite	Montmorillonite
Rocha	5.8	3.5	1.8	2.0
College	4.0	1.9	1.8	14.6
Basilica	4.1	1.5	2.3	14.4

**Table 3** Swelling strain values

Sample	Swelling strain/mm m <sup>-1</sup>
Basilica	0.03
College	11.02
Rocha	2.46

### Swelling strain

The average values obtained for each sample are presented in Table 3. As is observed, very different values were obtained for the three samples. The College stone presented a spectacular swelling strain. This value is seven times higher than the reported value of 1.5 mm/m, which is considered the critical value associated with fractures generated inside the stone [15]. The swelling strain value for Rocha stone is smaller than that obtained for College; however, it is higher than the critical value. The Basilica stone shows practically no swelling.

### FTIR

The band assignments were done according to the reports from Van der Marel and Beutelspacher [31]. The Basilica

sample presented characteristic bands of montmorillonite, at 3629 and 3427 cm<sup>-1</sup>, which correspond to the bonds (Mg, Al)–O–H and Al–O–H, respectively; the 3,236.6 cm<sup>-1</sup> band was assigned to water molecules tightly bonded to the mineral surface as a monolayer, and were observed the established bands for the bonds Si–O, at 1038 cm<sup>-1</sup>, and Si–O–Al, at 525 cm<sup>-1</sup>. In addition, a band corresponding to Si–O–Si bonds is observed at 1166 cm<sup>-1</sup>, as documented in Table 4. The sample did not present bands associated with bonds (Al, Fe)–O–H, at 878 cm<sup>-1</sup>; (Al, Mg)–O–H, at the range 845–835 cm<sup>-1</sup>; Si–O–Mg, at 467 cm<sup>-1</sup> or Si–O–Fe, at 450 cm<sup>-1</sup>; this suggests that the montmorillonite is poor in magnesium and iron and rich in aluminum.

The College sample also presented the characteristic bands of montmorillonite described for the Basilica sample, Table 4. In addition, and unlike the Basilica sample, this sample presented small shoulders assigned to bonds (Al, Mg)–O–H, at 844 cm<sup>-1</sup>, and Si–O–Mg, at 467 cm<sup>-1</sup>.

The Rocha sample presented bands of low intensity in the region from 3800 to 3400 cm<sup>-1</sup>. The main bands corresponded to illite, at 3624, 1098, 1022, 642, 530, and 470 cm<sup>-1</sup>. Other bands, at 1035, 911, 692, and 431 cm<sup>-1</sup>, can be assigned to halloysite. Finally, the bands at 3413, 1035, 878, and 525 cm<sup>-1</sup> can be assigned to montmorillonite.

The three samples presented one broad complex band in the range from 1200 to 900 cm<sup>-1</sup>; this suggests that the samples are amorphous, or a mixture of different clays. On the other hand, it is clear that quartz and feldspars present in the clay fractions were not totally removed from the bulk samples with the sedimentation process; strong bands at 796 and 777 cm<sup>-1</sup> and medium bands at ~588 and 510 cm<sup>-1</sup>, respectively, were observed.

**Table 4** Transmittance band values, wavenumbers in cm<sup>-1</sup>, from FTIR spectra of clay fractions

Basilica	3629m	3427m	1630 m	1388sh	797s	694m	638vw	588w
				1166sh	777s	525m		472s
				1098sh	724sh			427sh
				1035s				
				918sh				
College	3630m	3428m	1637m	1388vw	797s	694m	640sh	586w
				1164sh	776s			522m
				1102sh	729sh			467sh
				1035 s				419sh
				916 sh				
Rocha	3783w	3413w	1628vw	1139sh	796s	694m	642m	590m
				1095sh	777s			530m
				1035s	729sh			510w
				1019sh				470s
				911sh				431m

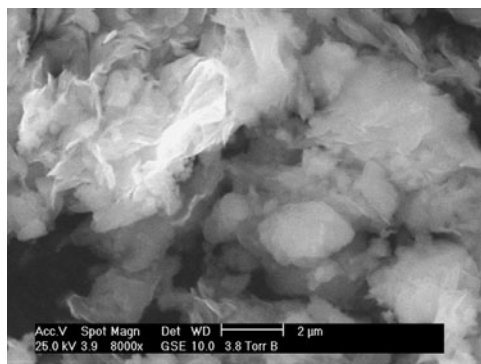


**Fig. 4** Micrograph of Basilica clay fraction

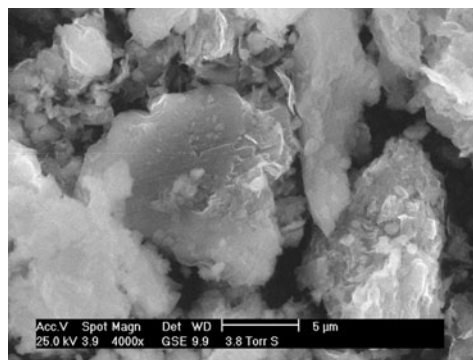


**Fig. 6** Micrograph of Rocha clay fraction

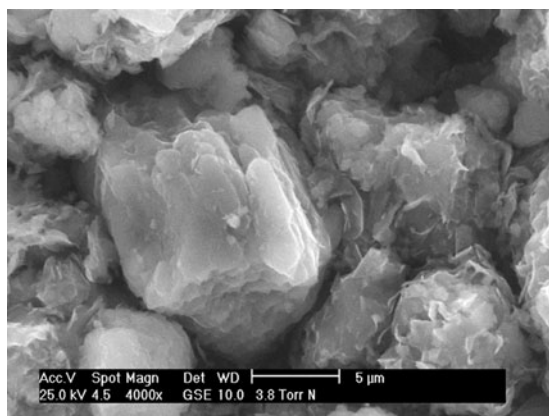


**Fig. 5** Micrograph of College clay fraction

In addition, spectra of prepared KBr disks, heated to 150 °C overnight, were obtained. In these spectra, only the Rocha clay fraction showed an additional weak band at  $3698\text{ cm}^{-1}$ , assigned to the most characteristic band of kaolinite in agreement with Madejová [32].

## ESEM

Most of the particles observed in the Basilica clay fraction were individual or conglomerate flakes with a “cornflake-like” inter-grown arrangement, and very small size amorphous material ( $<1\text{ }\mu\text{m}$ ). Some of the largest conglomerates have few crenulations with diffuse edges. In addition, a few platy crystals with a pseudo-hexagonal morphology, and several large crystals were observed as well, Fig. 4.

The College clay fraction is composed of grains with a size from 10 to 30  $\mu\text{m}$  and covered with flakes. It is clear that the flakes are formed on the surface of the grains because the flake edges tend to curl away from the grain surface. There were also some clusters of very small particles, between 0.5 and 1  $\mu\text{m}$  and some aggregates of thin

plates with a hexagonal morphology that suggests the presence of kaolinite crystals, Fig. 5.

Figure 6 illustrates an example of the different particles observed in the Rocha sample. This fraction showed a mixture of the morphologies observed in Basilica and College, grains covered with overlapping flakes, diffuse and poorly defined particles and small amorphous particles, 1–3  $\mu\text{m}$ . In addition, a few large fragments with clean surfaces were also observed.

## Discussion

### Identification of clays

#### *Basilica*

Although, observations by ESEM showed that most particles have the characteristic morphology of montmorillonite, the signals obtained by XRD are broad and of low intensity.

The montmorillonite content determined by thermal analysis is about 14%; however, the dehydroxylation peak obtained by DTA is wide and the maximum temperature is slightly lower than the corresponding temperature for the College clay fraction. According to Smykatz [33] the temperature of dehydroxylation of montmorillonites depends on the bond strength between cations and OH groups, lower for iron,  $\text{Fe}^{2+}/\text{Fe}^{3+} < \text{Al} < \text{Mg}$ . The temperature also decreases if there is disorder in the structure, and the size of the particles is very small [30].

The FTIR spectrum suggests that the montmorillonite contained is rich in aluminum with probably few isomorphic substitutions in octahedral and tetrahedral layers. These data together with the fact that cornflake aggregates have diffuse edges also suggest that the montmorillonite is in a state of transformation. This is probably the reason why the signal detected by XRD is broad and of low intensity.

The other phases, undetected by XRD, are poorly defined, suggesting that they would be in formation with a crystal size too small to be detected by XRD. On the other hand, the particles with pseudo-hexagonal morphology could correspond to kaolinite, detected by DTA and TG, while the amorphous particles observed probably correspond to halloysite.

### *College*

The curved flakes observed by ESEM and covering most of the grains were assigned to the mixed layers of illite and montmorillonite. They have been already identified by XRD and reported previously [34]. There were no elongated particles that correspond to the morphology reported for illite; therefore, it can be considered that the illite phase detected by thermal analysis is forming the clay interstratified mixed layer. For halloysite and kaolinite, no signals were obtained by XRD and FTIR. By ESEM, kaolinite particles were observed while smectite particles were not. This indicates: (1) the possible direct formation of kaolinite and illite–montmorillonite mixed layer from potassic-feldspar present in the sample. These data are supported in previous reports [35, 36], and (2) the illite–montmorillonite mixed layer is rich in montmorillonite, according to the percentages found by TG.

On the other hand, the percentage of clays calculated for this sample is similar to the percentage obtained for Basilica. The differences between these samples are in the crystallinity of the mixed layer illite–montmorillonite, the different morphology of particles, the presence of bands assigned to bonds Al–O–Mg and Si–O–Mg and the slight increase in temperature of dehydroxylation of montmorillonite. These variations can be explained in function of the different age of the monuments and the samples condition. According to the observations made by thin section petrography [26], the College sample showed some fractures and pores, and as a consequence, the possibility of ions removal is low. Therefore, the composition of new formed minerals is similar to the primary minerals [37]. By contrast, the Basilica bulk sample showed many irregular fractures and pores.

### *Rocha*

In this sample many small amorphous particles were observed by ESEM. This was reflected in the shape of DTA curves and also in the FTIR spectra and in the XRD signals. Petrographic data obtained previously showed that this stone has less fractures than Basilica and a salt crystals content greater than College but less

than Basilica. From these results, it is possible to consider that the new minerals were formed in a semi-open system, which resulted in the increase of halloysite formation. Similar to the College sample, curved flakes observed on the surface of grains were assigned to a mixed layer illite–montmorillonite detected by XRD. However, the sample has a high proportion of illite, determined by TG (5.8%) and small amounts of montmorillonite (2.0%). According to these results, it is considered that the mixed layer is rich in illite. By ESEM no other characteristic morphology was observed corresponding to the other phases detected by DTA and TG, halloysite, and kaolinite. It is possible to suggest that the small and amorphous particles observed correspond to these phases. These are probably in formative stages.

### Swelling behavior of samples

According to reports from the literature [15] swelling values above 0.15% can cause damage to stone materials free of pressure. Therefore, from the values obtained in the College and Rocha samples (1.1 and 0.246%, respectively), it is possible to associate damage by the swelling of clays in the monuments. The College sample came from one of the cornices. This area showed fractures, spalling, and the loss of large sections. Similar conditions were found in the Rocha monument. In contrast, although the Basilica sample came from the most deteriorated section of the monument, practically no swelling was observed.

The clays covering the grain surfaces were observed in College and Rocha by ESEM. Such clays form a layer surrounding grains in the stone, so their swelling is directly reflected in the expansion of the stone [14]. While many irregular fractures stuffed with material argillaceous were observed by thin section petrography in the Basilica sample. In addition, in the Basilica sample, it was observed that the fractures also contained a great amount of small salt crystals, while in the College sample were scarcely observed and in the Rocha sample less than in Basilica sample. Therefore, the concentration of ions in the samples is very different. To lower amount of ions surrounding the clay surfaces, the repulsion among the particles becomes bigger, giving place to the osmotic swelling [18]. Probably, this could explain the big difference obtained in the swelling measurements reported for the samples.

On the other hand, the swelling of the stone is very much smaller than that of the clay minerals themselves [18]. Therefore, the clay phases in College sample showed a very spectacular swelling capacity.

## Conclusions

It was identified and quantified, by thermal analysis, the clay phases of illite, montmorillonite, kaolinite, and halloysite in samples of volcanic tuffs. Such volcanic tuffs were used as building stones in three historic monuments located in the city of Guanajuato, Mexico. The presence of these clay phases was confirmed by XRD, FTIR, and ESEM.

Given the great similarity between the mineralogical compositions of the samples, the different proportions of clays present in each sample suggest that their formation is influenced largely by the monument microenvironment and the history of each one.

The values obtained in the measurements for swelling strain in bulk samples demonstrate the importance of the presence of clays in the monuments studied.

The data suggest that differences in swelling behavior of the samples are largely due to the location of the clays in the stone structure and to the content of salts.

**Acknowledgements** The authors are grateful to Professor George Wheeler for his assistance with separation of clays and XRD analysis. Also, they would like to thank Prof. George Scherer for swelling measurements. Veridiana Reyes-Zamudio is grateful to Consejo Nacional de Ciencia y Tecnología (Mexico), for the fellowship to perform PhD studies; and also, to Professor George Wheeler for the support and advice during research stays at Columbia University and the Scientific Department of the Metropolitan Museum of Art, New York (USA).

## References

- Funicello R, Heiken G, Levich R, Obenholzner J, Petrov V. Construction in regions with tuff deposits. In: Heiken G, editor. *Tuffs: their properties, uses, hydrology, and resources*. Colorado: The Geological Society of America; 2006. p. 119–26.
- Ostromov M, Garduño-Monroy VH, Carreon-Nieto H, Lozano-Santa Cruz R. Mineralogía y geoquímica de los procesos de degradación en monumentos históricos: primer acercamiento a un caso mexicano (Morelia, Michoacán). *Rev Mex Cienc Geol*. 2003;20:223–32.
- Grissom CA. The deterioration and treatment of volcanic stone: a review of the literature. In: Charola AE, Koestler RJ, Lomardi G, editors. *Lavas and volcanic tuffs*. Rome: International Center for the Study of the Preservation of Cultural Property; 1994. p. 3–29.
- Berner RA. A model of Atmospheric CO<sub>2</sub> over Phanerozoic Time. *Am J Sci*. 1991;291:339–76.
- Alonso E, Martínez L. The role of environmental sulfur on degradation of ignimbrites of the Cathedral in Morelia, Mexico. *Build Environ*. 2003;38:861–7.
- Simão J, Ruiz-Agudo E, Rodríguez-Navarro C. Effects of particulate matter from gasoline and diesel vehicle exhaust emissions on silicate stones sulfation. *Atmos Environ*. 2006;40:6905–17.
- Schiavon N. Kaolinisation of granite in an urban environment. *Environ Geol*. 2007;52:399–407.
- Kawano M, Tomita K, Shinohara Y. Analytical electron microscopic study of the noncrystalline products formed at early weathering stages of volcanic glass. *Clays Clay Miner*. 1997;45:440–7.
- Steindlberger E. Volcanic tuffs from Hesse (Germany) and their weathering behaviour. *Environ Geol*. 2004;46:378–90.
- Velde B, Meunier A. *The origin of clay minerals in soils and weathered rocks*. Berlin: Springer-Verlag; 2008.
- Srodon J. X-ray identification of randomly interstratified illite-smectite in mixtures with discrete illite. *Clay Miner*. 1981;16:297–304.
- Siegesmund S, Weiss T, Vollbrecht A. Natural stone, weathering phenomena, conservation strategies and case studies: introduction. In: Siegesmund S, Weiss T, Vollbrecht A, editors. *Natural stone, weathering phenomena, conservation strategies and case studies*. UK: Geological Society of London; 2003. p. 1–7.
- Veniale F, Setti M, Rodríguez-Navarro C, Lodola S. Procesos de alteración asociados al contenido de minerales arcillosos en materiales pétreos (Role of clay constituents in Stone decay processes). *Mater Constr*. 2001;51:163–82.
- Delgado Rodrigues J. Swelling behaviour of stones and its interests in conservation: an appraisal. *Mater Constr*. 2001;51:183–95.
- Jiménez-González I, Rodríguez-Navarro C, Scherer GW. Role of clay minerals in the physicochemical deterioration of sandstone. *J Geophys Res*. 2008; F02021. doi:10.1029/2007JF000845.
- Madsen FT, Müller-Vonmoos M. The swelling behaviour of clays. *Appl Clay Sci*. 1989;4:143–56.
- Foster MD. The relation between composition and swelling in clays. *Clays Clay Miner*. 1954;3:205–20.
- Jiménez-González I. PhD Thesis. Universidad de Granada; 2008.
- Rodríguez-Navarro C, Sebastian E, Doehne E, Winell WS. The role of sepiolite-paligorskite in the decay of ancient Egyptian limestone sculptures. *Clays Clay Miner*. 1998;46:414–22.
- Weiss T, Siegesmund S, Kirchner D, Sippel J. Insolation weathering and hygric dilatation: two competitive factors in stone degradation. *Environ Geol*. 2004;46:402–13.
- Wangler T, Scherer GW. Clay swelling mechanism in clay-bearing sandstones. *Environ Geol*. 2008;56:529–34.
- Wheeler G. *Alkoxysilanes and the consolidation of stone*. Los Angeles: Getty Publications; 2005.
- Scherer GW. Internal stress and cracking in stone and masonry. In: Konsta-Gdoutos MS, editor. *Monitoring and modeling concrete properties*. The Netherlands: Springer; 2006. p. 633–41.
- Stück H, Forgó LZ, Rüdrieh J, Siegesmund S, Török Á. The behaviour of consolidated volcanic tuffs: weathering mechanisms under simulated laboratory conditions. *Environ Geol*. 2008;56:699–713.
- Wendler R, Snethlage E. Moisture cycles and sandstone degradation. In: Baer NS, Snethlage R, editors. *Saving our architectural heritage: the conservation of historic stone structures*. Chichester: Wiley; 1997. p. 7–24.
- Reyes-Z V, Cervantes-Jáuregui J. In: *Proceedings of the 41st congress IUPAC—chemistry protecting health, natural environment and cultural heritage*, Torino, Italy. 5–11 August 2007.
- Shoval S, Gaft M, Beck P, Kirsh Y. Thermal behavior of limestone and monocrystalline calcite tempers during firing and their use in ancient vessels. *J Thermal Anal*. 1993;40:263–73.
- Cardiano P, Sergi S, De Stefano C, Ioppolo S, Piraino P. Investigations on ancient mortars from the Basilian monastery of Fragala. *J Therm Anal Calorim*. 2008;91:477–85.
- Duran A, Perez-Maqueda LA, Poyato J, Perez-Rodriguez JL. A thermal study approach to roman age wall painting mortars. *J Therm Anal Calorim*. 2010;99:803–9.
- Todor DN. *Thermal analysis of minerals*. England: Abacus Press; 1976.
- Van der Marel and Beutelspacher. *Atlas of infrared spectroscopy of clay minerals and their admixtures*. Amsterdam: Elsevier; 1976.



32. Madejová J. FTIR techniques in clay mineral studies. *Vib Spectrosc.* 2003;31:1–10.
33. Smykatz-Kloss W, Heide K, Klink W. Applications of thermal methods in the geosciences. In: Brown ME, Gallagher PK, editors. *Handbook of thermal analysis and calorimetry*, vol. 2: applications to inorganic and miscellaneous materials. Amsterdam: Elsevier; 2003. p. 451–594.
34. Morris KA, Shepperd CM. The role of clay minerals in influencing porosity and permeability characteristics in the Bridport Sands of Wytch Farm, Dorset. *Clay Miner.* 1982;17:41–54.
35. Papoulis D, Tsolis-Katagas P, Katagas C. Progressive stages in the formation of kaolin minerals of different morphologies in the weathering of plagioclase. *Clays Clay Miner.* 2004;52:275–86.
36. De la Fuente S, Cuadros J, Fiore S, Linares J. Electron microscopy study of volcanic tuff alteration to illite-smectite under hydrothermal conditions. *Clays Clay Miner.* 2000;48:339–50.
37. Meunier A, Sardini P, Robinet JC, Prêt D. The petrography of weathering processes: facts and outlooks. *Clay Miner.* 2007; 42:415–35.